Experimental validation of a 3D SPH model for the simulation of a dam-break event involving multiple fixed and mobile bodies

RAFFAELE ALBANO, DOMENICA MIRAUDA, AURELIA SOLE
School of Engineering
Università degli Studi della Basilicata
Via dell'Ateneo Lucano n.10, 85100 - Potenza
ITALY
albano.raffaele@tiscali.it; domenica.mirauda@unibas.it; aurelia.sole@unibas.it.

ANDREA AMICARELLI, GIORDANO AGATE
Department SFE
Ricerca sul Sistema Energetico RSE SpA
Via R. Rubattino n.54, 20134 - MIlano
ITALY
Andrea.Amicarelli@rse-web.it; Giordano.Agate@rse-web. it.

ANGELA CELESTE TARAMASSO
DICCA Dipartimento di Ingegneria Civile, Chimica ed Ambientale
Università degli Studi di Genova
via Montallegro 1 16145 Genova
ITALY
act@dicca.unige.it;

Abstract: - Fast-moving flows due to flash floods and/or dam-break events may often cause potential hazard to human beings and their proprieties in urban floodplains. Recently, flood risks related to solid bodies transport, such as vehicles, have become more and more common and, therefore, worth investigating.
These hydraulic phenomena are complex events difficult to analyze if not through numerical modeling. In order to validate the accuracy of the models, and to demonstrate their capabilities in reproducing this kind of phenomena, experimental tests are necessary.
In this paper, a dam break wave evolution involving two fixed structures and three mobile bodies is simulated with a 3D Smoothed Particle Hydrodynamics model and validated through laboratory experiments. The model is shown to accurately fit both the measures of flow depths, upstream the fixed obstacles, and the bodies' movements in time. Therefore, in order to study and mitigate the risks due to the floating bodies transport, the model could be used to support or, eventually, substitute laboratory experiments, which are expensive, difficult to perform and, in most cases, not completely repeatable.

Key-Words: - Laboratory experiments, Smoothed Particle Hydrodynamics model, floating bodies transport, flash food, dam-break event

1 Introduction

The occurrence of urban flooding due to flash floods has recently been increasing as a consequence of climate change. In addition, flash flooding as well as dam-break events often lead to extremely dangerous conditions along anthropized fluvial areas, thus causing deaths and losses of property, mostly due to short timescales and limited warning time.
For example, during the Rapid City flash flood, South Dakota, on June 9, 1972, a heavy rain caused a falling of up to 38 centimeters in less than six hours. The spillway at Pactola Dam, located upstream of Rapid City, plugged up with cars and house debris, causing the lake level to rise 3.66 meters ([3]).
Similarly, during the Boscastle flood, England, in August 2004, 115 vehicles were swept off by the floodwater; some of these were caught under a local bridge, blocking the flow path and finally causing collapse under the stress ([2]).
Hence, flash floods and/or dam-break flows may be considerably affected by the presence of such

ISBN: 978-960-474-376-6

artificial obstacles. In particular, in the case of dam-break events, the influence of such obstacles is amplified, especially in the first instants after the dam break and in the immediate vicinity of the dam ([1]). Large debris, including vehicles parked along the floodplains, could produce more severe damages and an increasing in loss of life, as happened in the 1976 Big Thompson flood, Colorado ([4], [5]).

For a better management of the enhanced flood risks, it is useful to assess the large floating bodies transport caused by dam-break events or flash floods in urban areas through numerical modeling.

Flood propagation in urban areas is often simulated by Computational Fluid Dynamics (CFD) models, able to characterize in detail complex phenomena such as the transport of solid structures, vehicles, tree trunks, etc., providing additional information that cannot be obtained from direct experimental observation ([8]).

Nonetheless, the traditional grid-based CFD models have shown some limitation when applied to fast flows in transitory regimes that involve fluid-structure interactions.

In this context, Smoothed Particles Hydrodynamics (SPH) models represent, instead, a mesh-less CFD technique particularly fit for the representation of free surface flow impact on fixed and mobile structures ([9], [10], [11], [12]), substituting the grid with a set of arbitrarily distributed nodes.

The main advantages of SPH concern the direct estimation of the free surface and the interfaces between fluids or phases - as defined by the positions of the numerical particles.

However, the SPH model is generally more time consuming than Eulerian CFD techniques, as the numerical stencil of each computational node is composed by around a hundred particles in 3D, instead of a tenth of cells for mesh-based models.

Nevertheless, the algorithm is suited to parallelization, noticeably reducing the negative effects of this shortcoming ([9], [6], [7]).

Conceptually, the method represents a particle technique, where each particle is considered as a computational node, based on an interpolation approach over the values of the surrounding - "neighbour" - particles. The functions and derivatives appearing in the balance equations of fluid dynamics are approximated using convolution integrals over a limited space (the kernel support V_h: a sphere of radius 2h, h being the kernel support size) around a generic computational node/particle (located at the position x_0), and weighted by an analytical smoothing function (or kernel: W).

In particular, the integral SPH approximation (SPH approximation in the continuum) of a generic function (f) is defined as:

$$\langle f \rangle_{I,\underline{x}_0} = \int_{V_h} fW dx^3 \qquad (1)$$

Applying the same operator to a generic derivative, computed along the spatial component x_i, and integrating by parts, the integral SPH approximation provides the following equation:

$$\left\langle \frac{\partial f}{\partial x_i} \right\rangle_{I,\underline{x}_0} = \int_{A_h} fWn_i dx^2 - \int_{V_h} f \frac{\partial W}{\partial x_i} dx^3 \qquad (2)$$

where *n* is the unity vector, locally normal to the boundary.

The discretisation of the volume integral in (2) should consider fluid particles (called "neighbouring particles") around the computational particle. Conversely, the surface integral in (2) should be computed over the boundary A_h of the kernel support.

Several SPH studies have so far dealt with the transport of solid bodies, driven by free surface or confined flows, mainly in 2D and with single 2-way interactions. In particular, [15] used the ghost particle method to model a 2D dynamics of a falling wedge into still water, while [16] the interactions between water surface waves and fixed cylinders through the use of the boundary force particles. With the same technique, [17] and [18] analyzed the fluid-body interaction terms to model a floating body, driven by surface waves (in 2D and 3D, respectively). [19] reproduced the transport of 2D bodies in confined visco-elastic flows, deriving a formulation similar to [13] for fluid-solid interactions, but introducing modifications to deal with shear stresses and to obtain a first-order consistency scheme. They also used repulsive forces, defined for body-body impingements. The same authors represented the transport of 2D bodies in confined flows in [20]. [21] modeled the 3D impact of a falling parallelepiped on still water, coupling a Finite Element Method code (solid modeling) with SPH fluid particles. Finally, [22] directly represented solid-solid interactions applying the equation that describes the collision of two rigid bodies in 3D (approximated using an SPH formalism) and providing qualitative validations.

In this paper, we validated the 3D SPH model, recently developed by [12], on laboratory experiments for multiple bodies transport in free surface flows.

ISBN: 978-960-474-376-6

2 Experimental tests

The 3D SPH model of [12] was validated on an experimental apparatus simulating a dam-break event, in scale 1:40, through the fast automatic opening of a mobile gate.

The wave front affected a link road in the immediate vicinity of the water reservoir, involving two fixed structures – buildings – and transporting three floating bodies –vehicles, finally impacting a down-flow wall.

The experimental tests were carried out in the Hydraulics Laboratory of Basilicata University, on a tilting flume with a rectangular cross section of 0.5m x 0,5m (Fig. 1).

The dimensions of the experimental domain are 2.500x0.500x0.500m^3 (Fig. 1), while each structure is 0.300x0.150x0.300m^3. The first fixed structure - Structure 1 - is at 1.40m from the left boundary of the reservoir, while the other fixed structure - Structure 2 – is at 1.950m, and they are at 0.020m and 0.060m away from the vertical boundary closest to them, respectively.

The three transported bodies are parallelepipeds with dimensions of 0.118x0.045x0.043m, m_B=0.025kg mass, and ρs=111kg/m3 density.

The bodies were initially at rest, and their centers of mass were located at 1.407m, 1.515m, and 1.622m away from the left boundary of the reservoir, and at 0.229m, 0.221m, and 0.213m from the right wall, respectively, being all at 0.0215m from the bottom.

The position of the bodies, representing the vehicles, complied with the steering kinematics equation for vehicles [23], and the literature criteria for parking design [23].

The experiment provided the water depths time evolution through two resistive gauges located upstream the fixed structures, as indicated by the points in magenta in Fig. 2, and the 3D floating bodies displacements through the image analysis of two Charge Coupled Device cameras (CCD). The space recorded by the cameras was limited to a portion of the channel, from 1.4m to 2.1m along the streamwise direction to the flow.

The bodies movements in time were obtained by two algorithms: the object extractor, using the threshold technique of [24], and the object tracker of the Matlab image processing library, able to recognize the positions on each image.

3 Validation

The numerical model reproduces the experimental apparatus in scale 1:1. In the numerical simulation, the gate begins to lift a t_0=0.00s, with a uniform vertical velocity w=0.11m/s until t=2.00s, when it stops.

The model solves the balance equations for the 3D dynamics of rigid bodies and involves fluid-body and solid-solid multiple interactions. The fluid-body interactions are modeled according to the boundary treatment introduced by [13], who validated the model for 2D frontiers with an imposed kinematics. Here, we have adapted it to handle free-slip conditions and used it for 3D body dynamics. The solid-solid interactions (body-body and body-boundary impingements) are modeled according to the SPH boundary force particles of [9]. We have modified it, in order to deal with low velocity impingements of entire solid bodies. The numerical scheme for body dynamics has been coupled this way with a Weakly Compressible Smoothed Particle Hydrodynamics (WC-SPH) model, which is based on the semi-analytic approach for the fluid-boundary treatment ([14]).

As it is possible to observe from the Figure 3, the numerical flow depths are in good agreement with the experimental ones. Only in the decreasing phase, after the peak, an underestimation of the experimental data as opposed to the numerical results is noted, due to the reflection of the wave front against the fixed structures.

To evaluate the reliability of the numerical flow depths, the Nash–Sutcliffe model efficiency coefficient is here estimated:

$$\eta = 1 - \left(\sum_{i=1}^{n} \left(h_{ei} - h_{ni} \right)^2 \Big/ \sum_{i=1}^{n} \left(h_{ei} - \overline{h}_e \right)^2 \right) \qquad (1)$$

where h_e is the experimental value of the free surface height, $\overline{h}_e$ is the mean of the experimental values and h_n is the value that come from the numerical model.

The value of the efficiency coefficient is around 0.7 for the surface height at the up-flow faces of Structure 1 and is around 0.5 for the surface height at the up-flow faces of Structure 2, due to the highest overestimation of the wave front descendent part in the numerical data. However, the peaks are well estimated (Fig. 3).

The numerical results well represent the experimental data, even when comparing the bodies' displacements (Fig. 4 and 5).

In particular, Figure 4 provides qualitative comparisons between the numerical results and the experimental data.

ISBN: 978-960-474-376-6

Figure 1 - Experimental apparatus. Left: overview of the apparatus; right: plan section of the apparatus).

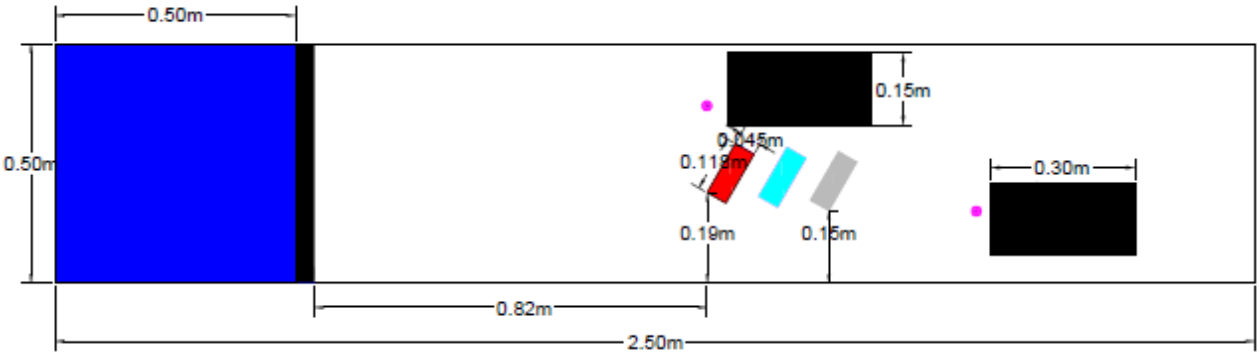

Figure 2 - Experimental domain

As Figure 4a shows, the wave front impacts, at t=1.00s, the first fixed structure and moves its upwind face upwards. At the same time, it transports the first floating body, and then the others, down-flow.

At t=1.40s, the third floating body – Body 3, i.e. the one positioned farther from the gate, is the first one that impacts the second fixed structure (Figure 4b and Figure 4c) and it is deviated laterally, after having been lifted in the air due to the impact. Subsequently, the other two floating bodies (Body 1 and 2) impact Structure 2 being lifted up in air and falling down into water, remaining in the up-wind part of Structure 2 (Figure 4d).

At around t=1.80s, Body 1 begins to overpass the upwind face of the downwind Structure 2, while Body 3 is almost at the end of the domain (Figure 4d).

Body 2 remains in the upwind part of the domain, i.e. upwind Structure 2, but, finally, it begins to overpass this structure. Then, the wave front and the wave surface are reflected by the down-flow boundary and slowly transport the floating bodies far from the down-flow boundary.

The good agreement between the experimental and numerical bodies trajectories, underlined qualitatively above, was demonstrated quantitatively through the comparison of the relative error percentages.

In particular, Figure 5a shows the relative error percentages for the values of the x-coordinate of the body centre of mass, considering only the time interval when the bodies are in motion. These percentages are less than 5% for most part of the data: for Body 1, over than 72%; for Body 2, over than 83%; and for Body 3, over than 48%. The highest absolute error percentage is less than 15%.

The numerical values of the z-coordinate of the body centre of mass are less precise than the ones on the x-coordinate (Figure 5b). However, the relative error percentages are less than 10% for almost the 50% of the data, and only in the 10% the error value is over 20%.

Considering these values, the model results to be able to reconstruct the body trajectories fairly well. Nevertheless, the numerical trajectories cannot accurately reproduce the impact of Body 3 on the second structure and anticipate the exit of Body 1 from the recirculation zone, up-flow the same structure.

ISBN: 978-960-474-376-6

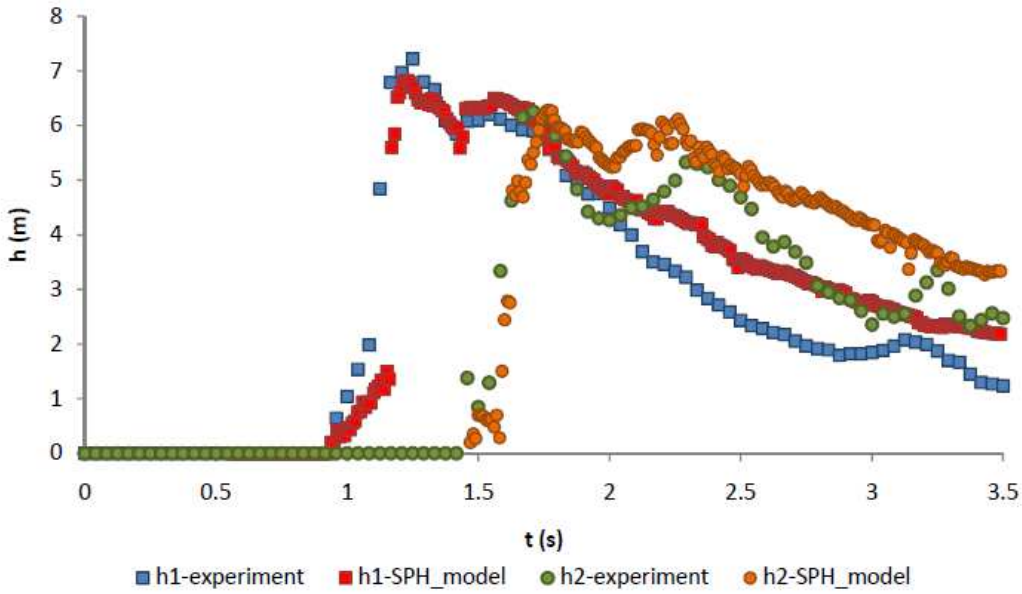

Figure 3 - Dam break with bodies transport: validations over experimental values. Time evolution of the free surface height (h1) at the up-flow faces of obstacle 1 (up-flow) and time evolution of the free surface height (h2) at the up-flow faces of the obstacle 2 (down-flow).

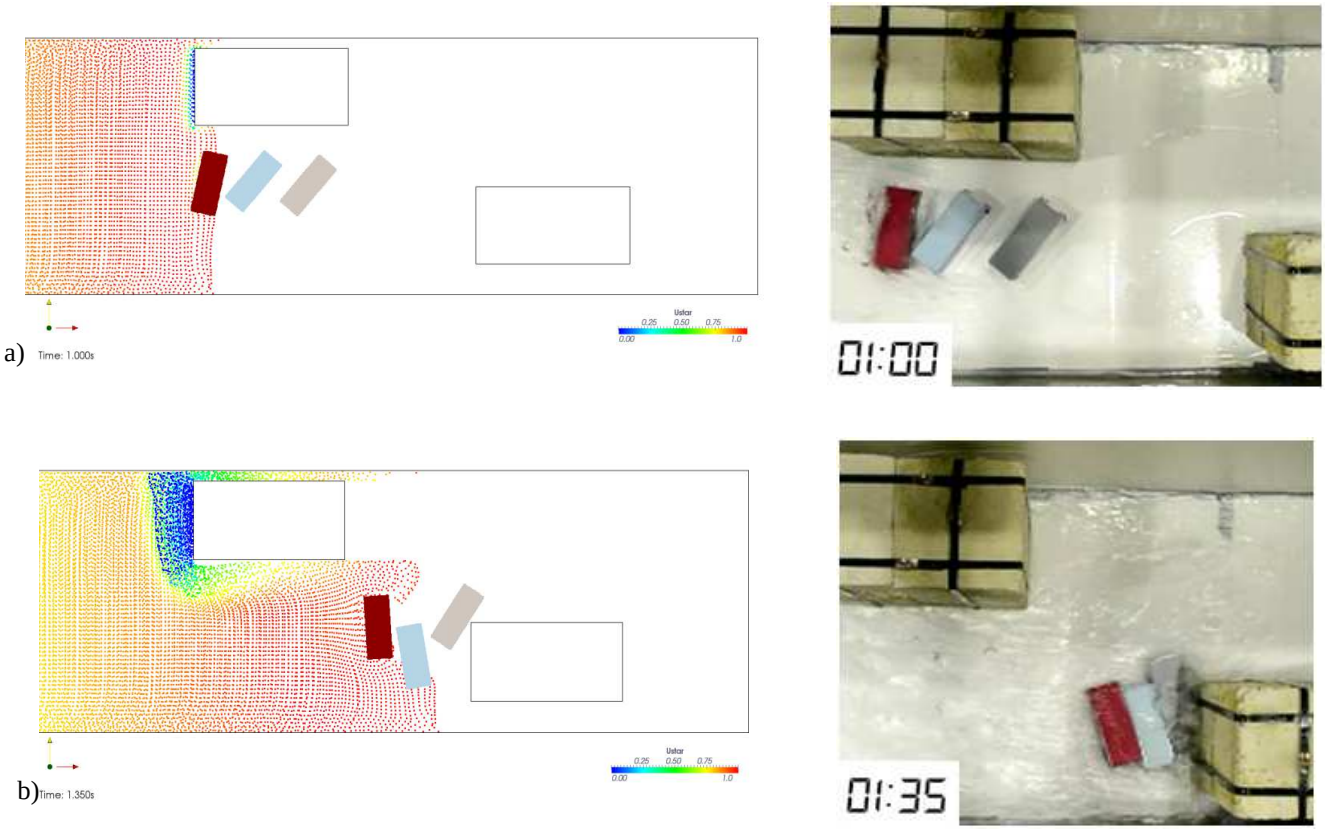

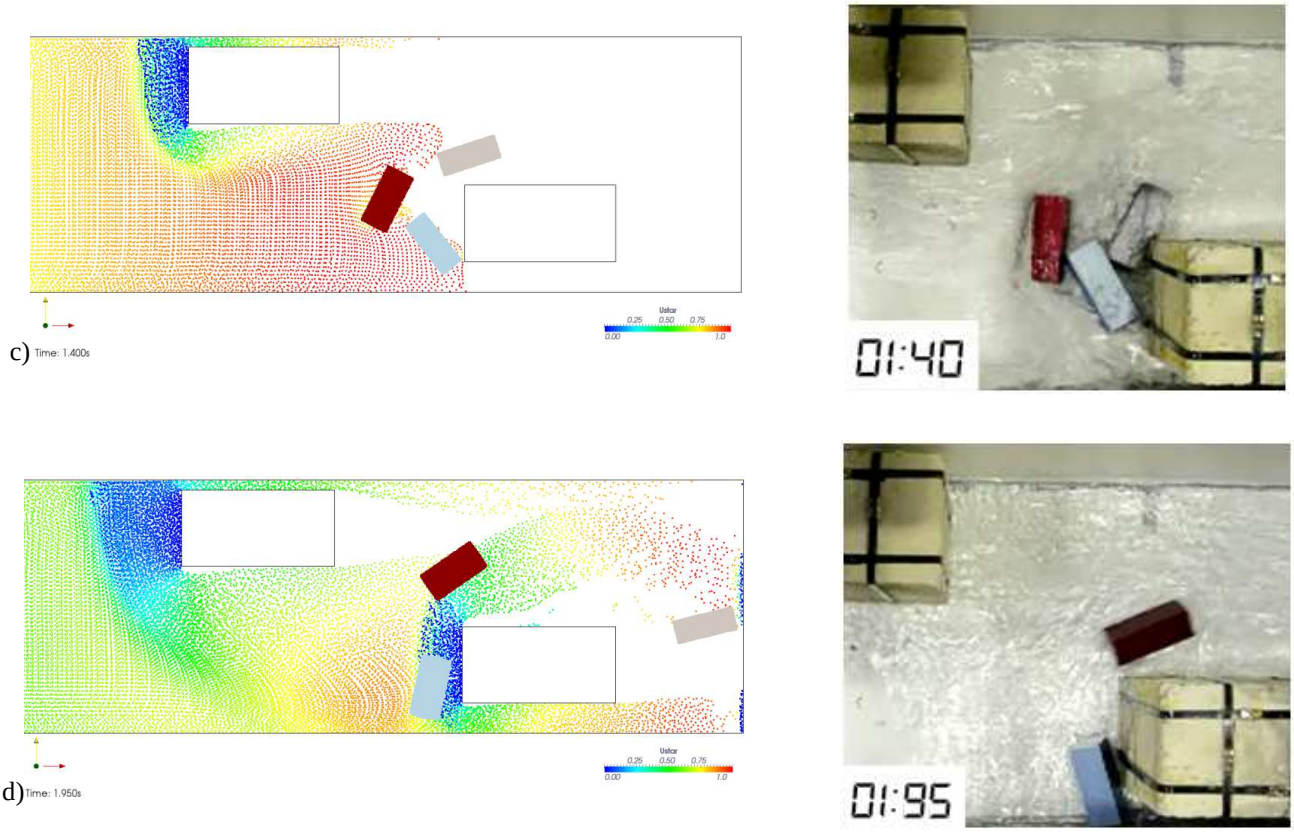

Figure 4. Comparisons between the results of the SPH model and the experimental tests a) at t=1.00s; b) at t=1.35s; c) at 1.40s; d) at 1.95s

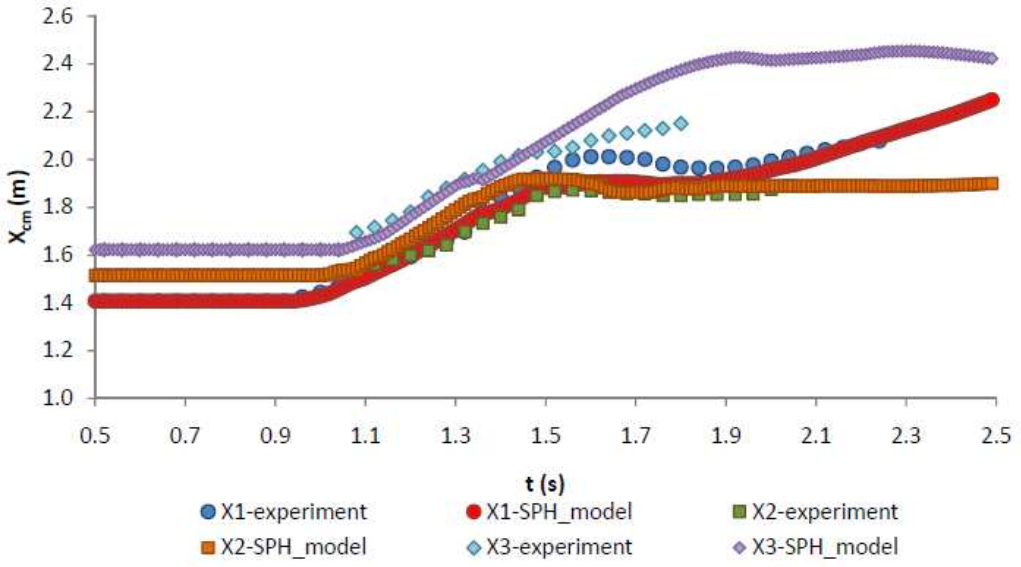

a)

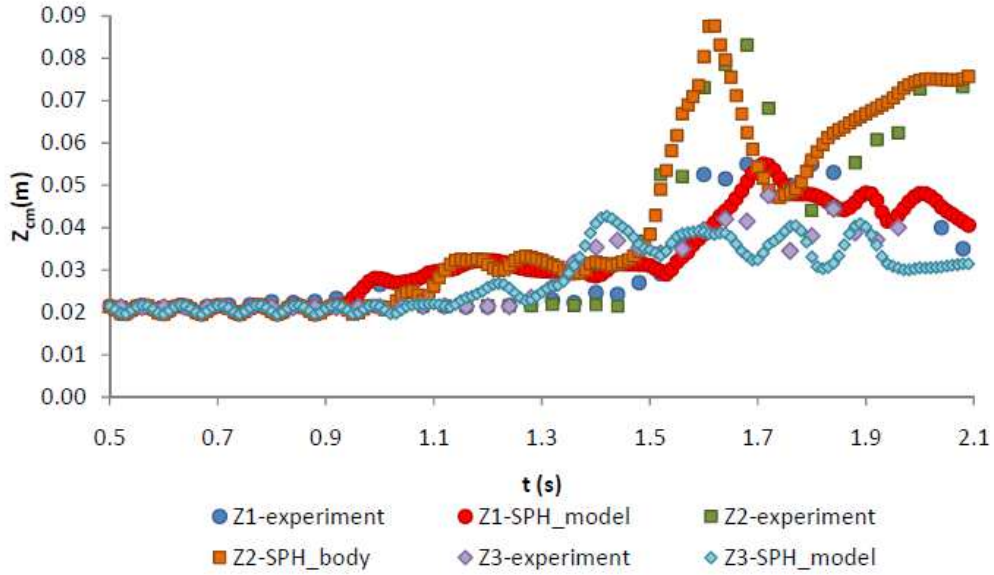

b)

Figure 5 - Dam break with bodies transport: validations over experimental values. Top (a): time evolution of the x-coordinate of the centre of mass of the bodies; down (b): time evolution of the z-coordinate of the centre of mass of the bodies

However, the vertical positions of the bodies are correctly represented, even when Body 2 impacts Structure 2, is lifted up with the rising wave front and then falls down. In the numerical model, the exact estimation of the bodies' position, near the impact zone of the first fixed structure, is affected by the limitation of the image detection process, caused by the bodies' rapid changes of orientation and also by the water flows covering them.

4 Conclusion

In this work, we validated the Smoothed Particle Hydrodynamics model of [12] on laboratory experiments, which simulate the behavior of a dam-break event involving buildings and vehicles in an urban floodplain.

The reliability of the model in reproducing the 3D transport of floating bodies was demonstrated both in terms of relative error percentage and in terms of efficiency index, i.e. the Nash–Sutcliffe model efficiency coefficient.

The obtained results underline the suitability of the SPH model to analyze complex phenomena, like fast-moving flows (flash floods and/or dam-break events), involving multiple fixed and mobile structures. This is especially true when the standard approaches fail, such as the linear and second-order wave diffraction theory, which does not represent highly nonlinear effects associated with extreme waves.

The SPH model, thus, allows individuating the measures and intervention strategies to mitigate the risks connected to the evolution of such phenomena.

Nonetheless, future validation processes of the model will be necessary, also through the use of data observed in field.

Acknowledge

The contributions of the two authors belonging to RSE SpA were financed by the Research Fund for the Italian Electrical System under the Contract Agreement between RSE SpA and the Italian Ministry of Economic Development - General Directorate for Nuclear Energy, Renewable Energy and Energy Efficiency, stipulated on July 29, 2009, in compliance with the Decree of November 11, 2012.

References:

[1] Alcrudo F. and Mulet J., Description of the Tous Dam break case study (Spain), *Journal of Hydraulic Research* Vol. 45 Extra Issue, pp. 45–57, 2007

[2] Teo F.Y., Xia J., Falconer R.A., Lin B., Experimental study on the interaction between vehicles and floodplain flows, *International Journal River Basin Management* Vol.10, No. 2, pp. 149-160, 2012

[3] Gruntfest, E., Ripps, A., Flash floods: warning and mitigation efforts and prospects, *Floods, London, Routledge*, 1: 377–390, Ed: D. Parker, 2000.

[4] Gruntfest, E., *What people did during the Big Thompson flood*, Natural Hazard Center, Boulder, Working Paper No. 32, 1977.

[5] Gruntfest, E., Flash floods in the United States, *Storms, London, Routledge*, Eds: J.R. Pielke & S.R. Pielke, pp. 192–206, 2000.

[6] Liu G.R. & Liu M.B., Smoothed Particle Hydrodynamics: A Meshfree Particle Method, *World Scientific*, 2003, ISBN: 981-238-456-1.

[7] Violeau D., *Fluid Mechanics and the SPH Method - Theory and Applications*, Oxford University Press, 2012, ISBN-10: 0199655529

[8] Gomez-Gesteira M., Rogers B.D., Violeau D., Grassa J. & Crespo A.J.C., Foreword: SPH for free-surface flows. *Journal of Hydraulic Research* 48:sup1, pages 3-5, 2010.

[9] Monaghan J.J., Smoothed particle hydrodynamics; *Rep. Prog. Phys*. 68, 1703–1759, 2005.

[10] Liu X, Xu H, Shao S, Lin P. An improved incompressible SPH model for simulation of wave structure interaction. *Computers and Fluids* 2013; 71:113-123

[11] Vaughan GL. The SPH equations for fluids. *International Journal for Numerical Methods in Engineering* 2009; 79:1392–1418

[12] Amicarelli A., R.Albano, D. Mirauda, G. Agate, A. Sole, R. Guandalini; A Smoothed Particle Hydrodynamics model for 3D solid body transport in free surface flows. *IJNMF International Journal for Numerical Methods in Fluids*, in revision.

[13] Adami S., Hu X.Y., Adams N.A., A generalized wall boundary condition for smoothed particle hydrodynamics, *Journal of Computational Physics*, 231, 7057–7075, 2012.

[14] Di Monaco A., Manenti S., Gallati M., Sibilla S., Agate G., Guandalini R., SPH modeling of solid boundaries through a semi-analytic approach, *Engineering Applications of Computational Fluid Mechanics*, 5, 1, 1–15, 2011.

[15] Oger G, Doring M, Alessandrini B, Ferrant P. Impulse-based rigid body interaction in SPH. *Journal of Computational Physics* 2006; 213:803–822.

[16] Monaghan JJ, Kos A, Issa N. Fluid motion generated by impact; *Journal of Waterway, Port, Coastal and Ocean Engineering* 2003; 129:250–259.

[17] Omidvar P, Stansby PK, Rogers BD, Wave body interaction in 2D using smoothed particle hydrodynamics (SPH) with variable particle mass, *International Journal for Numerical Methods in Fluids* 2012; 68:686–705.

[18] Omidvar P., Stansby P.K, Rogers B.D., SPH for 3D floating bodies using variable mass particle distribution, *International Journal for Numerical Methods in Fluids* 2012

[19] Hashemi M.R., Fatehi R., Manzari M.T., SPH simulation of interacting solid bodies suspended in a shear flow of an Oldroyd-B fluid. *Journal of Non-Newtonian Fluid Mechanics* 2011; 166:1239– 1252.

[20] Hashemi M.R., Fatehi R., Manzari M.T., A modified SPH method for simulating motion of rigid bodies in Newtonian fluid flows. *International Journal of Non-Linear Mechanics* 2012; 47:626– 638.

[21] Anghileri M., Castelletti L.M., Francesconi E., Milanese A., Pittofrati M., Rigid body water impact - experimental tests and numerical simulations using the SPH method. *International Journal of Impact Engineering* 2011; 38:141-151.

[22] Seungtaik O., Younghee K., Byung-Seok R. Impulse-based Boundary Force (IBF). *Computer, animation and virtual worlds* 2009: 20:215–224.

[23] Pacejka H.B., *Tyre and Vehicle Dynamics*. Elsevier Science & Technology, 2005.

[24] Gonzalez R.C., Woods R.E., *Digital Image Processing, Pearson International Edition*